Springer

Journal of
Mechanical
Science and
Technology

Journal of Mechanical Science and Technology 23 (2009) 372~380

www.springerlink.com/content/1738-494x
DOI 10.1007/s12206-008-0921-8

Applications of fiber models based on discrete element method to string vibration †

Junyoung Park[1] and Namcheol Kang[2,*]

[1]*School of Mechanical Engineering, Kumoh National Institute of Technology, 1 Yangho, Gumi, Gyeongbuk, South Korea 730-731*
[2]*School of Mechanical Engineering, Kyungpook National University, 1370 Sankyuk-dong, Buk-gu, Daegu, South Korea, 702-701*

(Manuscript Received July 22, 2008; Revised August 13, 2008; Accepted September 18, 2008)

Abstract

This study applies DE (discrete element) computational method to the dynamic problems of a vibrating string. The DE method was originally initiated to analyze granular materials and now it has expanded to model fabric dynamics which is of interest in a number of applications including those that manufacture or handle textiles, garments, and composite materials. Owing to the complex interactions between each discrete element, simple circular geometric rigid model has been used in the conventional DE method. However, in order to analyze the slender shape and flexibility of materials such as fabrics or strings, longer and flexible geometric models, named as fiber models, was developed. The fiber model treats a series of connected circular particles, and further can be classified as being either a RF (rigid fiber) or a CFF (completely flexible fiber) model. To check the feasibility of those models, dynamic problems were solved and it is found that the fiber models accurately simulate the dynamic and vibration behaviors of horizontally or vertically placed strings.

Keywords: Completely flexible fiber model; DEM (Discrete Element Method); Rigid fiber model; String vibration

1. Introduction

The dynamics of fabrics, for example in a washing machine, is very complex not only because of geometric complexity but also because of composition of dissimilar materials. In addition, since fabrics can have different thicknesses and can be subjected to large bending deformations, models including such details are too complex to represent the dynamic behaviors in practical applications. Furthermore, although such fabric elements are successfully modeled, the computations would be essentially impractical due to a large number of interactions between each element in a system.

Despite appearing seemingly unrelated, the dynamics of a fabric in a rotating drum for example, have many similarities with that of discrete element in ball mills. The particle dynamics occurring within a ball mill have been widely studied by the DE (discrete element) method [1-4]. A ball mill is a device used to grind or crush particulates and commonly consists of a rotating drum partially filled with grinding media, typically steel balls, and the material to be comminuted.

The DE method is similar in many respects to physical force-based models but it includes more detailed contact force models and is typically used to investigate the dynamics of discrete particle systems. There are several types of DE model including the soft-particle and hard-particle approaches. In general, the majority of DE simulations rely upon the soft-particle method because it provides the gradual contact when the elements interact each other.

Although the conventional DE model predicts

† This paper was recommended for publication in revised form by Associate Editor Hong Hee Yoo

*Corresponding author. Tel.: +82 53 950 7545, Fax.: +82 53 950 6550
E-mail address: nckang@knu.ac.kr

accurately the dynamics of particles, however, essentially it is not appropriate to simulate the slender shape or the flexibility of materials due to its simple shape. For this reason, two fiber models were developed in this study to simulate long-shaped flexible elements such as a vibrating string. These include modeling fabric elements as rigid fibers (RF) and completely flexible fibers (CFF); where the bending stiffness of the first is infinite whereas that of the second vanishes.

Furthermore, the rigid fiber and completely flexible fiber models were applied to the dynamics problems of a vibrating string. Three well known vibration problems were solved by the fiber models in the DE simulation. According to the good agreement with analytic solutions of the those three case studies, it is found that the developed RF and CFF models in DE simulation accurately predicts the dynamic and vibration characteristics and can be expanded to the study of complex and nonlinear vibrating systems.

2. Discrete element method

2.1 Discrete element approach

The DE method has been used extensively for investigating the dynamics of granular materials for the last twenty years. In DE modeling, the material under investigation is treated as a collection of discrete objects or elements. Several types of DE algorithms exist including the soft-particle and hard-particle approaches, Monte Carlo models, and cellular automata. The majority of DE simulations, however, rely upon the soft-particle method since it offers flexibility when including element interactions, can model long-lasting and multiple-particle contacts, and is based on deterministic physics rather than probability.

In the soft-particle approach method, forces acting on each element are governed by appropriate force laws at each instant. The accelerations of the elements are determined by Newton's second law and new particle states are then found by integrating the resulting equations of motion in time. This process is repeated until the final state, for example a maximum time limit, is reached. A flowchart of the DE algorithm is illustrated in Fig. 1. Although the algorithm is straightforward, the DE approach can be computationally intensive because a large number of particles are often used in the simulations. In a ball mill study which is one of the typical applications of DE method, it has been shown that two-dimensional DE simulations predict three-dimensional dynamics well [4]. Hence, the present study considers only two-dimensional systems.

2.2 Contact forces and parameters

Typically, the forces acting on elements include both body and surface forces. The body force acting on element i is the gravitational force, or weight, $\boldsymbol{F}_{G,i}$, given by

$$\boldsymbol{F}_{G,i} = m_i \mathbf{g} \tag{1}$$

where m_i is the mass of i-th element and $\mathbf{g}$ is the gravity which acts at the center of mass of the element. The surface forces used in the present DE simulations include only contact forces between elements.

Quantifying the contact force between elements can be one of the most complex parts of DE modeling. In the soft-particle approach, the contact force is determined by the amount of overlap during contact. This overlap represents the surface deformation occurring when real materials come into contact. The amount of the overlap and the relative speed of the impact are often used to determine the resulting contact force.

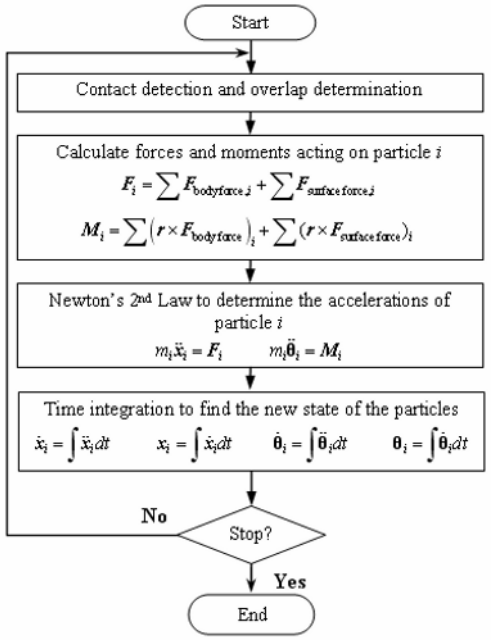

Fig. 1. Flowchart of the discrete element simulation algorithm.

Further, the contact force is subdivided into normal and tangential components. The normal component acts in the direction that is perpendicular to the plane defined by the intersection of the two elements, *i* and *j*. This direction is signified by the unit vector, $\mathbf{n}_{ji}$. On the contrary, the tangential force component acts in the direction perpendicular to the normal direction defined by the unit vector as shown in Fig. 2.

Three different normal contact force models can be utilized in the DE method such as the damped linear spring model [1], a non-linear hysteretic spring model [5], and the hysteretic (or latched) linear spring model [6]. In these models damped linear spring, which is composed of an elastic spring and a dashpot, is commonly used to calculate the normal and tangential contact forces as the schematic diagrams shown in Fig. 3. In this model, the normal spring force is generated by the repulsive elastic spring and damping force is by the dashpot which dissipates energy during the contact. Therefore, the normal contact force that *j*-th particle exerts on *i*-th particle, $\boldsymbol{F}_{n,ji}$ is written as

$$\boldsymbol{F}_{n,ji} = [-k_n \alpha_{ji} + \nu_n (\Delta \dot{\boldsymbol{x}}_{c,ji} \cdot \mathbf{n}_{ji})]\mathbf{n}_{ji} \tag{2}$$

where k_n and ν_n are the spring constant and damping coefficient between particles, respectively. In addition, α_{ji} is the amount of overlap between the two particles, and $\Delta \dot{\boldsymbol{x}}_{c,ji}$ is the velocity of a particle relative to the other particle at the contact point. Finally, $\mathbf{n}_{ji}$ is the unit vector pointing from the center of *i*-th particle to the center of *j*-th particle.

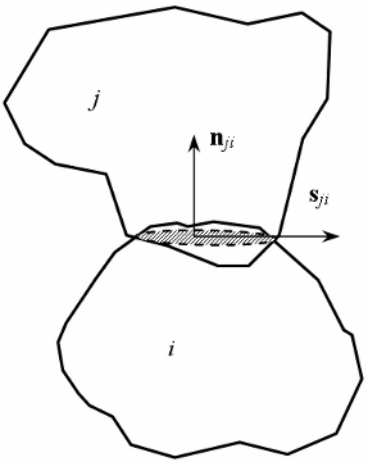

Fig. 2. The normal and tangential directions of the contact force.

Parameters used in normal contact force of Eq. (2) can be calculated as following. The overlap, α_{ji}, between two circular particles is

$$\alpha_{ji} = (r_j + r_i) - \left| \boldsymbol{x}_j - \boldsymbol{x}_i \right| \tag{3}$$

where $\boldsymbol{x}_i$ is the position vector indicating the center of mass of *i*-th particle and r_i is the radius of the *i*-th particle (see Fig. 4). No contact occurs if $\alpha_{ji} < 0$ in the conventional DE model. The unit normal vector pointing from the center of *i*-th particle to the center of *j*-th particle, $\mathbf{n}_{ji}$, can be written as

$$\mathbf{n}_{ji} = \frac{\boldsymbol{x}_j - \boldsymbol{x}_i}{|\boldsymbol{x}_j - \boldsymbol{x}_i|} \tag{4}$$

Also, the unit tangential vector, $\mathbf{s}_{ji}$, is normal to $\mathbf{n}_{ji}$ and points in the direction of the relative tangential velocity. Finally, the velocity of *j*-th particle relative to *i*-th particle at the contact point, $\Delta \dot{\boldsymbol{x}}_{c,ji}$, is

$$\Delta \dot{\boldsymbol{x}}_{c,ji} = (\dot{\boldsymbol{x}}_j - \dot{\boldsymbol{\theta}}_j \times r_j \mathbf{n}_{ji}) - (\dot{\boldsymbol{x}}_i - \dot{\boldsymbol{\theta}}_i \times r_i \mathbf{n}_{ji}) \tag{5}$$

where $\dot{\boldsymbol{\theta}}_i$ and r_i are the angular velocity and the radius of *i*-th particle, respectively.

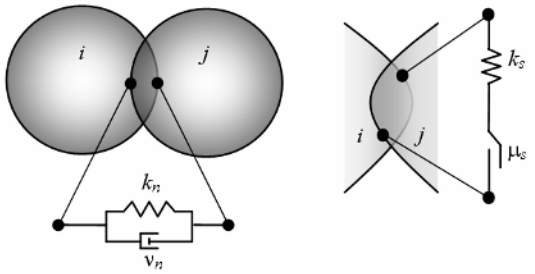

Fig. 3. Schematic diagrams of the normal and tangential contact forces in damped linear spring model.

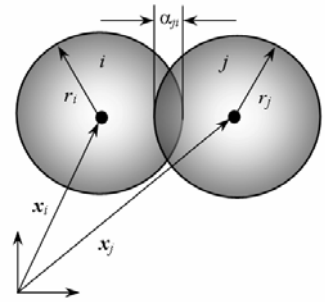

Fig. 4. Geometric configuration of two particles when overlapped.

The normal spring stiffness and damping coefficient are determined by the coefficient of restitution for the impact between two particles and by the allowed amount of overlap during the collision. For the damped linear spring model, the normal damping coefficient has relation to the spring stiffness and coefficient of restitution such as

$$\nu_n = \sqrt{\frac{4m'k_n}{1+\beta^2}} \tag{6}$$

where $m' = (m_i^{-1} + m_j^{-1})^{-1}$ is the equivalent mass of the colliding particles, $\beta = \pi/\ln\varepsilon$ where ε is the coefficient of restitution during the collision [7]. Also, the linear spring stiffness is found by limiting the maximum overlap during the collision to 1% of the minimum particle radius, $r_{\min}$, and written as for a typical impact velocity, V

$$k_n = m'\left[\frac{V}{0.01r_{\min}}\exp\left(-\frac{\tan^{-1}\beta}{\beta}\right)\right]^2 \tag{7}$$

Campbell observed that a maximum overlap of 1% of the particle radius is sufficient to avoid measurement errors resulting from excluded area effects [8]. In this study, because the deformation and collisions of fabrics are very dissipative, the baseline coefficient of restitution is set to 0.1.

Tangential force is also generated during contact and it is modeled as a linear spring in series with a sliding friction element in linear spring model (refer to Fig. 3). The spring force provides elastic tangential response while the sliding friction element provides dissipation. The tangential force exerted on i-th particle due to contact with j-th particle acting in the tangential direction, $\boldsymbol{F}_{S,ji}$, is given by

$$\boldsymbol{F}_{s,ji} = \begin{cases} -\int_{t_0} k_s \Delta\dot{\boldsymbol{x}}_{c,ji}\cdot\mathbf{s}_{ji}dt\,\mathbf{s}_{ji} \\ \qquad if\ \ \mu_s|\boldsymbol{F}_n| > \left|\int_{t_0} k_s\Delta\dot{\boldsymbol{x}}_{c,ji}\cdot\mathbf{s}_{ji}dt\right| \\ -\mu_S|\boldsymbol{F}_n|\mathbf{s}_{ji} \\ \qquad if\ \ \mu_s|\boldsymbol{F}_n| \le \left|\int_{t_0} k_s\Delta\dot{\boldsymbol{x}}_{c,ji}\cdot\mathbf{s}_{ji}dt\right| \end{cases} \tag{8}$$

where k_s and μ_s are the tangential spring stiffness and friction coefficient, respectively, t_0 is the time at which the contact was initiated, and $\boldsymbol{F}_n$ is the normal force for the contact. The tangential spring is active when the spring force is smaller than the frictional tangential force. However, when the friction force is smaller than the spring force, extension is adjusted so that it provides a force equivalent to the sliding friction force. For large tangential spring stiffnesses and small friction coefficients, the sliding friction element engages early in the contact and the tangential spring stiffness has little effect on the contact dynamics. Previous analytical and experimental studies have found that the ratio of the tangential spring stiffness to the effective normal spring stiffness should be $1 \le k_s/k_n \le 1.5$ [1, 9-10]. For the current simulations the baseline tangential-to-normal spring stiffness ratio is assumed to be unity. It is also reported that the friction coefficients of dry textiles are between 0.3 and 1.5, according to the experimental results performed by Carr et al. [11].

2.3 Geometric models

Conventional DE method employs circular particles or spherical ones as geometric models. However, because the conventional model is not capable of simulating the slender shape or the flexibility of materials due to its simple shape, fiber models were developed.

2.3.1 Rigid fiber model

The rigid fiber (RF) model is composed of a rigid array with inter-connected circular particles (see Fig. 5). Forces and moments acting on the fiber are due to the forces acting on the intra-fiber particles. Although this model allows for the slender shape of materials, it

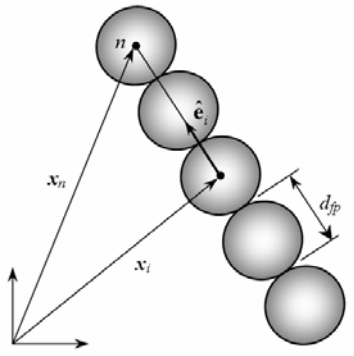

Fig. 5. Illustration of the rigid fiber model with geometric configuration.

does not include the effects of fabric flexibility. Therefore, this model is not investigated in detail in this study, but it is instructive in the sense of understanding the evolution of the DE models.

The intra-fiber particles are maintained at fixed positions aligned along a straight line relative to one another, and the absolute position of *n*-th particle in an intra-fiber $\boldsymbol{x}_n$ is given by

$$\boldsymbol{x}_n = \boldsymbol{x}_i + d_{fp}\left[(n-1) - \tfrac{1}{2}(N-1)\right]\hat{\mathbf{e}}_i \tag{9}$$

where, $\boldsymbol{x}_i$ is the location of the center at *i*-th intra-fiber, d_{fp} is the diameter of intra-fiber particles, N is the total number of elements in the intra-fiber structure, and $\hat{\mathbf{e}}_i$ is a unit vector pointing the axis of the fiber. In addition, the total mass of the fiber is

$$m_{fiber} = \sum_{n=1}^{n=N} m_n \tag{10}$$

By the application of parallel axis theorem, the moment of inertia of the fiber is written as

$$I_{fiber} = \sum_{n=1}^{n=N}\left\{\tfrac{1}{10} + \left[(n-1) - \tfrac{1}{2}(N-1)\right]^2\right\} m_{fiber} d_{fp}^2 \tag{11}$$

The baseline diameter of an intra-fiber particle is chosen such that the total area of the fiber (= $N\,\pi\,d_{fp}^2/4$) is equal to that of the area of a conventional circular particle.

2.3.2 Completely flexible fiber model

The completely flexible fiber (CFF) model incorporates both high aspect ratio and flexibility effects. Like the RF model, the CFF model consists of a series of circular particles linked together to form a fiber; however, unlike the RF model the centers of an intra-fiber particle are connected by springs so that they can have a relative motion in the intra-fiber. While in the RF model the forces and moments acting on the center of mass of the intra-fiber are calculated, the CFF model instead tracks the forces acting on each individual intra-fiber particle and does not apply these forces to the center of mass of the intra-fiber.

A linear damped spring is used to model the force between intra-fiber particle centers. Breen observed that a linear relationship for intra-fiber particle contact is valid for small deformations [12]. The spring constant and damping coefficient are chosen using the same analysis described in the previous section. No tangential springs are included between intra-fiber particles.

2.4 Integration of the governing equations

The forces acting on particles in the system were described in Section 2.2. Applying Newton's 2nd law, the accelerations of a particle (or rigid fiber) are calculated by

$$m_i \ddot{\boldsymbol{x}}_i = \sum \boldsymbol{F}_i \tag{12}$$

$$I_i \ddot{\boldsymbol{\theta}}_i = \sum \boldsymbol{M}_i \tag{13}$$

where m_i and I_i are the mass and moment of inertia of *i*-th particle (or rigid fiber), respectively. The accelerations are integrated in time using Euler's method with a fixed time step, Δt, to determine new states of the particle. In order to accurately integrate the resulting equations of motion, the time step is set to one-tenth the smallest period of motion which corresponds to the rotational motion of a particle in contact with the maximum number of particles that can surround the particle [13].

3. Application of Fiber Models

3.1 Rigid Fiber Model

The RF model simulation results are compared against the analytical solution for a rigid bar colliding with a fixed plate (see Fig. 6). The dynamics of a rigid bar impacting a surface can be found in a number of dynamics textbooks [14]. Assuming that the contact is frictionless, gravity can be neglected, and zero initial angular velocity, the angular velocity of the bar after the collision will be

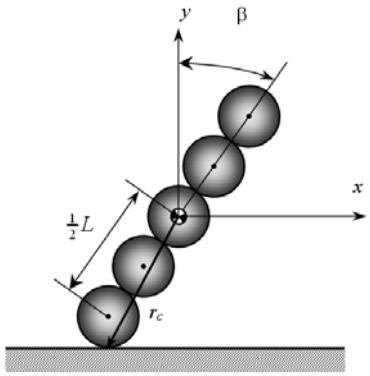

Fig. 6. Schematic of a rigid fiber colliding with a fixed plate.

$$\dot{\theta}_z^+ = \frac{M\left(\frac{L}{2}\sin\beta\right)(1+\varepsilon)}{I + M\left(\frac{L}{2}\sin\beta\right)^2} \cdot V_{y,CM}^- \tag{14}$$

where $V_{y,CM}^-$ is the center of mass y-velocity before the collision, M is the bar mass, ε is the coefficient of restitution for the collision, L is the bar's length, β is the angle between the y-axis and the bar prior to impact, and I is the bar's moment of inertia. The bar's center of mass y-velocity after the collision is:

$$V_{y,CM}^+ = -\varepsilon V_{y,CM}^- + \left(\frac{L}{2}\sin\beta\right)\dot{\theta}_z^+ \tag{15}$$

Table 1. Properties of the rigid fiber.

Parameter	Value
Mass of fiber, mf [kg]	0.443
Number of particles, N	5
Mass of a particle, mp [kg]	0.0886
Length of fiber, L [m]	0.0425
Restitution coefficient, e	0.9
Diameter of particle, d [m]	0.0106
Velocity before collision, V0 [m/s]	-2.0

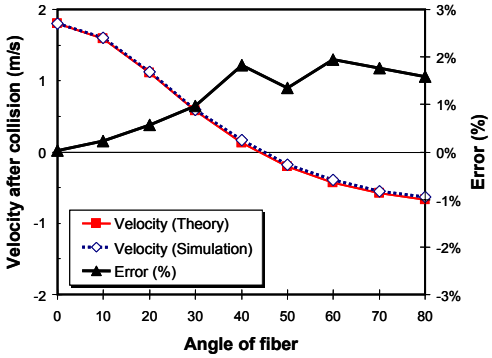

Fig. 7. Velocity and error of the rigid fiber after collision.

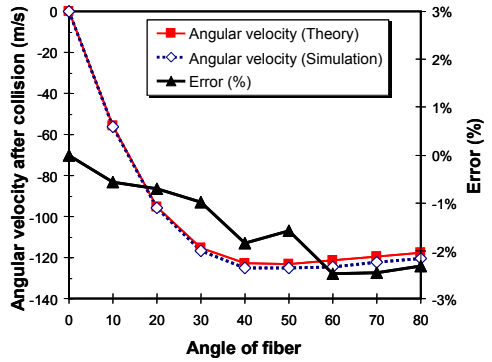

Fig. 8. Angular velocity and error of the rigid fiber after collision.

The RF simulation results for $V_{y,CM}^+$ and $\dot{\theta}_z^+$ are plotted in Fig. 7 and Fig. 8 respectively, along with the analytical predictions as a function of the initial bar angle. The parameters used here are listed at Table 1. The error generally increases with increasing bar angle and reaches a maximum of approximately 2%. The agreement between the two results indicates that the DE method correctly simulates the motion of a rigid, large aspect ratio object.

3.2 Completely flexible fiber model

Dynamic characteristics of a vibration string were analyzed by the CFF model of the DE method. First, the response of a flexible fiber fixed at both ends was compared to that of a string model. The classic linear string analytical model assumes that only small transverse motions ($A << L$ where A is the maximum displacement of the string and L is the string length, refer to Fig. 9) occur and that the change in tension with deflection can be ignored. The governing equation for the linear plucked string problem, so-called wave equation, is written in dimensionless variables

$$\frac{\partial^2 z'}{\partial t^2} = \frac{\partial^2 z'}{\partial x'^2} \tag{16}$$

where z' (= z/L) is the dimensionless transverse displacement, t' ($=\sqrt{\rho L^2/T}\cdot t$ where ρ is the string mass per unit length and T is the string tension) is time, and x' is the longitudinal direction (along the axis of the undeformed string, $x' = x/L$).

A very restrictive assumption to the linear wave equation is that the displacements must be very small compared to the length of the string. However, since the CFFs model used in the simulation can behave with very large deflections, it is directly applicable to a non-linear string problem. Assuming that the string

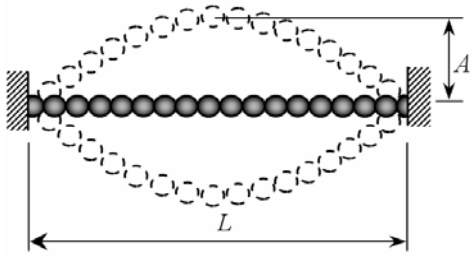

Fig. 9. Schematic of the vibrating string by CFF model.

mode shapes are sinusoidal, the dimensionless non-linear string equation, so-called Kirchhoff equation, becomes Duffing equation such as

$$\ddot{z}' + (m\pi)^2 z' + \frac{EA}{4T_0}(m\pi)^4 z'^3 = 0 \tag{17}$$

where z' is the dimensionless deflection along the transverse direction of the string (= z/L), m is an integer, E is the Young's modulus of the string, A is the cross-sectional area of the string, and T_0 is the initial tension acting on string. Although the solution to this nonlinear ordinary differential equation can be written in terms of a series solution, in this study, MATLAB was used to get a numerical solution.

The simulations are performed for a fixed fiber length with different number of particles in the range between 13 and 49. Also, to compare the effect of large deflections, maximum displacement of the vibrating string is increased up to 10% of the string length. In the computation, the spring constant between intra-fiber particles is not equal to that of the overall fiber Young's modulus. Instead, they are related by

$$k_{fiber} L = k_{particle}(N-1)/L \tag{18}$$

where k_{fiber} is the spring constant for the overall fiber, $k_{paricle}$ is the spring constant between intra-fiber particles, and N is the total number of particles in the fiber. Figure 10 shows the error of vibrating frequency calculated by CFF model and non-linear string one. As the number of particles is increased, the errors are monotonically decreased and remain less than 2% over two orders of magnitude difference in initial amplitude.

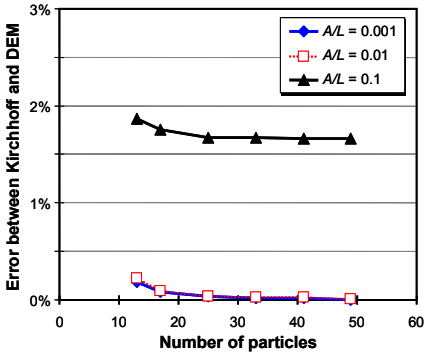

Fig. 10. The errors of a vibrating string in frequency with respect to the number of particles when computed by the CFF model.

The vibration of a vertically hanging string was also studied by the CFF model to check the feasibility of DE method. Considering the mass of a hanging string fixed at top, the general form of boundary value problem is written as [15]

$$\frac{d}{dx}\left[\rho g x \frac{dU(x)}{dx}\right] + \rho\omega^2 U(x) = 0 \tag{19}$$

where, ρ is the mass per length of the string, g is gravity, ω is the eigenvalue, and U (x) is the transverse displacement of the string. It is well known that the eigenfunctions of Eq. (19) are the Bessel function of zeroth order, i.e.,

$$U_n(x) = J_0\left(k_n\sqrt{\frac{x}{L}}\right) \tag{20}$$

and the corresponding period of n-th mode is

$$T_n = \frac{4\pi}{k_n}\sqrt{\frac{L}{g}} \tag{21}$$

where, L is the length of the string and k_n is the n-th positive root of $J_0(x)$.

The period of first four modes shown in Fig. 11 are simulated by DE method, and the errors of each mode are plotted in Fig. 12. All errors are monotonically decreased and further are converged certain values, as the number of particles is increased. It is interesting that the error of the 2nd mode is smaller than that of the 1st mode, however, the errors are all within 5% for a sufficient number of particles in the CFF model.

DE simulation results of vibrating strings ensure that the CFF model can be applicable to vibration problems as well as dynamic ones. Further, it is

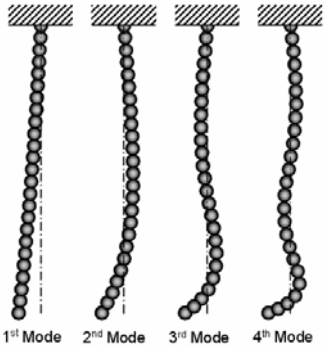

Fig. 11. First four modes of a vertically hanging string.

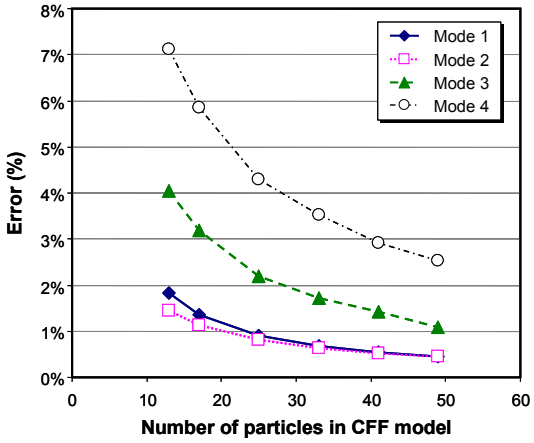

Fig. 12. The errors of a hanging string in period with respect to the number of particles when computed by the CFF model.

expected that the structure having bending rigidity such as a beam also can be analyzed by introducing PFF (partially flexible fiber) model, although it has not been developed yet.

4. Conclusions

The discrete element computational method was introduced and applied to dynamic problems. For the simulation of long shaped structure, two fiber models, rigid fibers (RF) and completely flexible fibers (CFF), were developed and applied to the analysis of dynamic problems such as a string vibration. Through the in-depth studies of three different cases, it is found that the fiber models of the DE method accurately predict the dynamic and vibration characteristics of horizontally or vertically placed strings.

References

[1] P. A. Cundall and O. D. L. Strack, A discrete numerical model for granular assemblies, *Geotechnique*, 29 (1) (1979) 47-65.

[2] C. S. Campbell and C. E. Brennen, Computer simulation of granular shear flows, *Journal of Fluid Mechanics*, 151 (1985) 167-188.

[3] A. Acharya, A distinct element approach to ball mill mechanics, *Communications in Numerical Methods in Engineering*, 16 (2000) 743-753.

[4] P. Cleary, Modelling comminution devices using DEM, *Int. J. Numer. Anal. Meth. Geomech.*, 25 (1) (2001) 83-105.

[5] C. M. Van Wyk, Note on the compressibility of wool, *Journal of the Textile Institute*, 36 (1946) T285-T292.

[6] O. R. Walton and R. L. Braun, Viscosity, granular-temperature, and stress calculations for shearing assemblies of inelastic frictional disks, *Journal of Rheology*, 30 (5) (1986) 949-980.

[7] C. R. Wassgren, *Vibration of granular materials*, Ph.D Thesis, California Institute of Technology, Pasadena, CA, (1997).

[8] C. S. Campbell, Computer simulation of rapid granular flows, *Proc. 10th US National Congress of Appl. Mech.*, (1986) 327-338.

[9] R. D. Mindlin and H. Deresiewicz, Elastic spheres in contact under varying oblique forces, *Journal of Applied Mechanics*, 20 (1953) 327-344.

[10] N. Maw, J. R. Barber and J. N. Fawcett, The oblique impact of elastic spheres, *Wear*, 38 (1) (1976) 101-114.

[11] W. W. Carr, J. E. Posey and W. C. Tincher, Frictional characteristics of apparel fabrics, *Textile Research Journal*, 58 (3) (1988) 129-136.

[12] D. E. Breen, D. H. House and M. J. Wozny, A particle-based model for simulating the draping behavior of woven cloth, *Textile Research Journal*, 64 (11) (1994) 663-685.

[13] D. N. Fernando, *Size segregation in granular beds subject to continuous and discrete oscillations*, M.S. Thesis, Purdue University, West Lafayette, IN, (2001).

[14] J. L. Meriam and L. G. Kraige, *Engineering Mechanics-Dynamics*, John Wiley & Sons, (2002).

[15] D. Yong, String, chains and ropes, *SIAM Review*, 48 (4) (2006) 771-781.

Junyoung Park received B.S. and M.S degrees in Mechanical Engineering from Kyungpook National University in 1996 and 1998, respectively. He then went on to receive his Ph.D. degree from Purdue University in 2003. Dr. Park is currently an assistant professor at the School of Mechanical Engineering at Kumoh National Institute of Technology in Gumi, Korea. Dr. Park's research interests are in the area of nano technology, particle technology, and analysis of pedestrian flow.

Namcheol Kang received B.S. and M.S degrees in Mechanical Engineering from KAIST and Seoul National University in 1992 and 1994, respectively. He then went on to receive his Ph.D. degree from Purdue University in 2004. Dr. Kang is currently an assistant professor at the School of Mechanical Engineering at Kyungpook National University in Daegu, Korea. Dr. Kang's research interests are in the area of dynamics, vibration and stability of a multi-scale mechanical system.